A New Type of Fast-Switching Dual-Mode Ferrite Phase Shifter

WILLIAM E. HORD, SENIOR MEMBER, IEEE, CHARLES R. BOYD, JR., FELLOW, IEEE AND DANIEL DIAZ

Abstract—**A new type of dual-mode phase shifter which uses a transversely magnetized variable field section is described. The device retains the features of the conventional dual-mode phase shifter—low insertion loss, moderate amplitude modulation, adequate frequency bandwidth, simple physical geometry—which allow it to be considered for use in two-dimensional scanning arrays. However, because of the transverse magnetizing field, the shorted-turn resistance is increased, which results in either reduced switching time or reduced switching energy when compared with the conventional dual-mode unit which utilizes a longitudinal magnetizing field.**

I. INTRODUCTION

THE DUAL-MODE phase shifter is shown conceptually in Fig. 1. The conventional dual-mode phase shifter uses the interaction of circularly polarized waves with longitudinally magnetized ferrite. For this design, the circulators of Fig. 1 are realized by permanent-magnet quadrupole field quarter-wave plate sections on either end of the variable field section. These quarter-wave plate sections convert linear polarization nonreciprocally to circular polarization and vice versa. A more detailed description is available in the literature [1], [2]. The new design of interest here uses a transversely magnetized ferrite-filled waveguide to realize the nonreciprocal phase shifters of Fig. 1. There are two major differences between the new design and the conventional dual-mode design:

1) The RF field propagating through the phase shift section is linearly polarized rather than circularly polarized.
2) The transverse magnetic bias field reduces the switching shorted-turn damping time constant.

Fig. 2 shows block diagrams of the longitudinal-field dual-mode phase shifter and two new realizations using the transverse field section. Fig. 2(b) allows operation with linearly polarized energy, while Fig. 2(c) is designed for circularly polarized waves. The "nonreciprocal polarizers" consist of 45° Faraday rotators at either end of the phase shift section in Fig. 2(b), while quadrupole field magnetic quarter-wave plates are used for the realization of Fig. 2(c).

The geometry of the transverse-field phase shifter is given in Fig. 3. A four-piece latching yoke is arranged to provide a quadrupole bias field in the microwave ferrite. A

Manuscript received April 6, 1987; revised July 17, 1987.

The authors are with the Microwave Applications Group, Santa Maria, CA 93455.

IEEE Log Number 8717122.

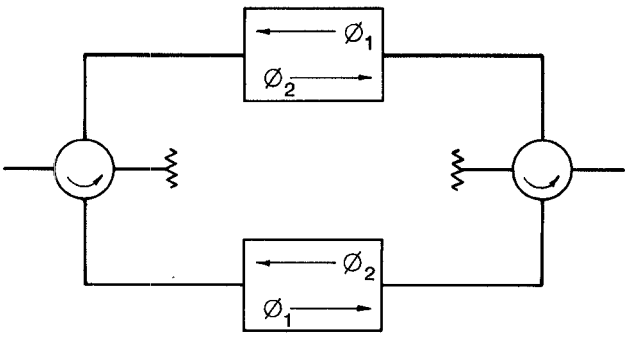

Fig. 1. Basic concept of the dual-mode ferrite phase shifter.

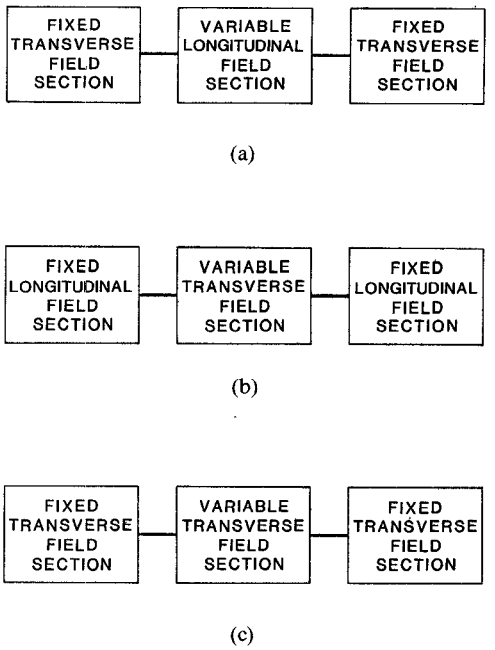

Fig. 2 Block diagram of dual-mode ferrite phase shifters. (a) Conventional dual-mode phase shifter. (b) The dual circuit of the conventional dual-mode phase shifter. (c) Another realization of the dual circuit.

y-polarized TE_{11} mode will exhibit different propagation constants for waves traveling in the $+z$ direction and the $-z$ direction. However, the symmetry is such that an x-polarized TE_{11} mode traveling in the $-z$ direction will have the same propagation constant as a y-polarized TE_{11} mode traveling in the $+z$ direction. The analysis given below closely parallels that of an earlier paper [3] which has not been widely distributed.

0018-9480/87/1200-1219$01.00

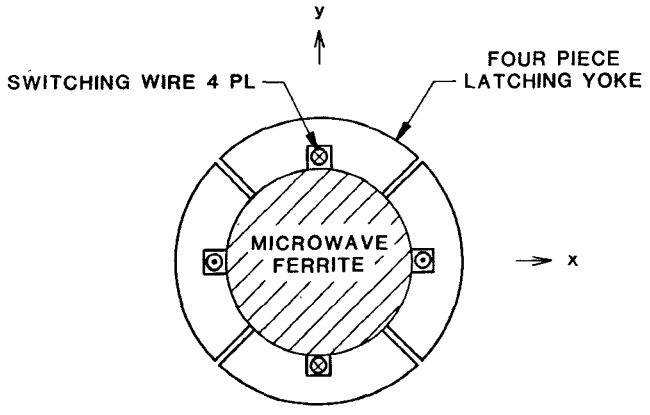

Fig. 3. Geometry of transverse field section.

II. RF Design Considerations

For a fully filled guide with transverse magnetization, the nonreciprocal differential phase shift $\Delta\phi$ is given by a relationship of the form

$$\Delta\phi = A\phi_0 \frac{f_c}{f}\frac{\kappa}{\mu} \tag{1}$$

where κ and μ are effective values of the permeability tensor for the magnetized ferrite, f_c is the cutoff frequency of the waveguide, f is the operating frequency, ϕ_0 is the insertion phase for a TEM wave propagating through the same length in the same medium, and A is a proportionality factor accounting for the relative effectiveness of the waveguide and bias field distributions. For example, A can be computed as equal to $4/\pi$ for a simple rectangular waveguide with equal and opposite uniform bias field level over the right and left halves of the guide. The mathematics leading to (1) have been derived on the basis of a transmission line equivalent-circuit model [4].

The insertion phase ϕ_0 can be expressed as

$$\phi_0 = \beta_0 l_\rho = \frac{360 f\sqrt{\mu_r \epsilon_r}}{c} l_\rho \tag{2}$$

with l_ρ defined as the length of the phase shift section; furthermore,

$$f_c = \frac{c}{\lambda_c \sqrt{\mu_r \epsilon_r}} \tag{3}$$

and for a circular waveguide $\lambda_c = 1.705D$, giving

$$\Delta\phi \cong 211A \frac{l_\rho}{D}\frac{\kappa}{\mu} \text{ degrees} \tag{4}$$

where D is the guide diameter.

When the rod is magnetized by a weak applied field, κ and μ can be approximated by [5]

$$\kappa \simeq \frac{M}{M_s}\frac{\omega_m}{\omega} \tag{5}$$

$$\mu = \mu_i + (1-\mu_i)\frac{\tanh\left(1.25\dfrac{M}{M_s}\right)}{\tanh 1.25} \tag{6}$$

where μ_i is the initial permeability, given by

$$\mu_i = \frac{1}{3} + \frac{2}{3}\sqrt{1 - \frac{(\omega_m)^2}{\omega}}\,. \tag{7}$$

If the applied field is large enough to saturate the rod completely, then κ and μ are more appropriately taken as

$$\kappa \simeq \frac{-M}{M_s}\left(\frac{\omega\omega_m}{\omega_0^2 - \omega^2}\right) \tag{8}$$

$$\mu = 1 + \frac{\omega_0\omega_m}{\omega_0^2 - \omega^2}\,. \tag{9}$$

In the above equations, ω is the operating radian frequency, ω_m is the material characteristic radian frequency, equal to the product of the gyromagnetic ratio and the saturation moment, and ω_0 is the resonance frequency given by Kittel's equation:

$$\omega_0 = \sqrt{\{\gamma H_0 + (N_x - N_z)\omega_m\}\{\gamma H_0 + (N_y - N_z)\omega_m\}}\,. \tag{10}$$

Here γ is the gyromagnetic ratio, H_0 is the externally applied field (z-directed), and N_x, N_y, and N_z are demagnetizing factors for the ferrite shape.

The phase shift sections of concern here are ideally designed to operate up to the "knee" of the magnetization curve to achieve maximum available phase shift. This peak operating point does not apparently conform to either the "weak-bias" or "strong-bias" case described above. However, experimental studies have yielded the following observations:

1) The coefficient A is numerically equal to about 1.23.
2) The "weak-bias" model fits experimental data reasonably well for $M/M_s \leqslant 0.25$. Above this level, a smooth transition begins toward the "strong-bias" model.
3) The "strong-bias" model gives a good fit to experimental data for M/M_s values near the "knee" of the magnetization curve.

Proceeding on this basis, take $\gamma H_0 = \omega_m M/M_s$ in (10) and note that for a long rod transversely magnetized, with the x direction along the rod axis,

$$N_x = 0 \qquad N_y = N_z = \tfrac{1}{2}. \tag{11}$$

Then substitute into (10) to get

$$r \equiv \frac{\omega_0}{\omega_m} = \sqrt{\frac{M}{M_s}\left(\frac{M}{M_s} - \frac{1}{2}\right)}\,. \tag{12}$$

Now it is possible to form the ratio κ/μ by substituting back into (8) and (9) after some manipulation obtain

$$\frac{\kappa}{\mu} \simeq \frac{M}{M_s}\frac{m}{1 - m^2 r(1+r)} \tag{13}$$

where $m \equiv \omega_m/\omega$ and r is defined by (12) above. Then

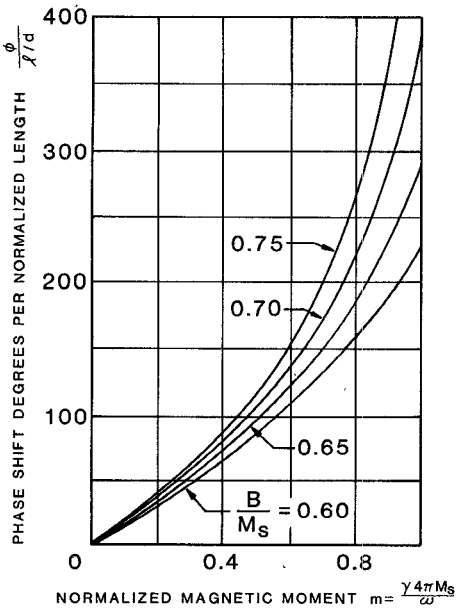

Fig. 4. Performance of differential phase shift section.

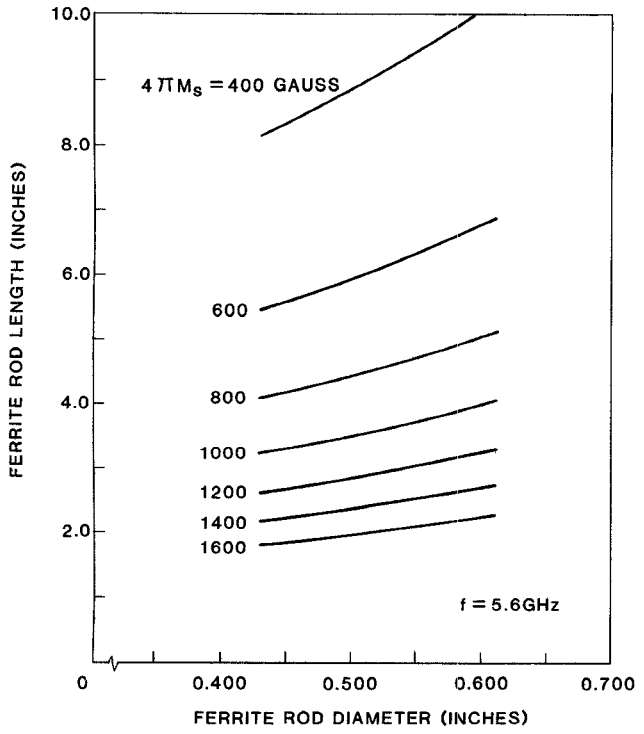

Fig. 5. *C*-band transverse-field dual-mode phase shifter ferrite rod design data.

using $A=1.23$, (4) for $\Delta\phi$ becomes

$$\Delta\phi = 260\frac{l_\rho}{D}\frac{M}{M_s}\frac{m}{1-m^2r(1+r)}. \tag{14}$$

Normalized curves relating maximum differential phase shift to m and the M/M_s ratios have been plotted in Fig. 4 using this relationship.

The general form of (4) and (14) shows that for fixed values of all other parameters, the length of the phase shift section will be proportional to the ferrite rod diameter. Fig. 5 indicates this relationship for a *C*-band design using

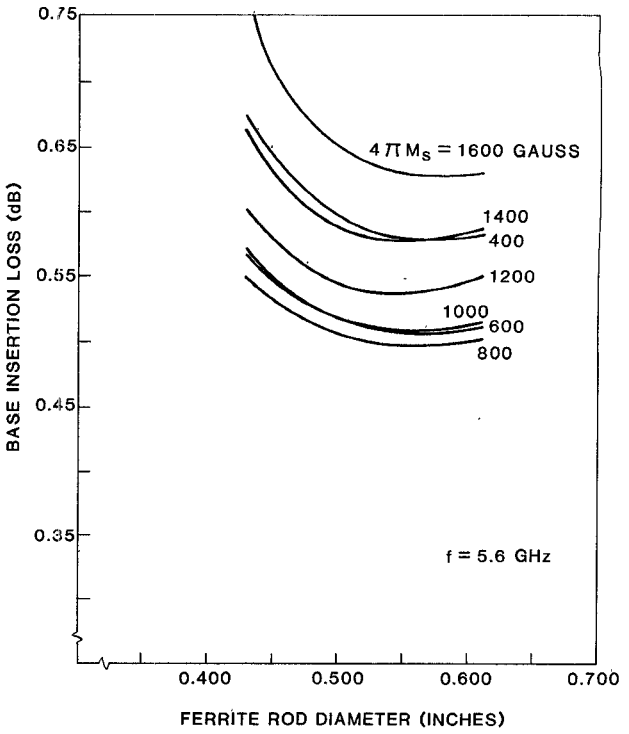

Fig. 6. *C*-band transverse-field dual-mode phase shifter loss dependence on rod diameter for various ferrite saturation moments.

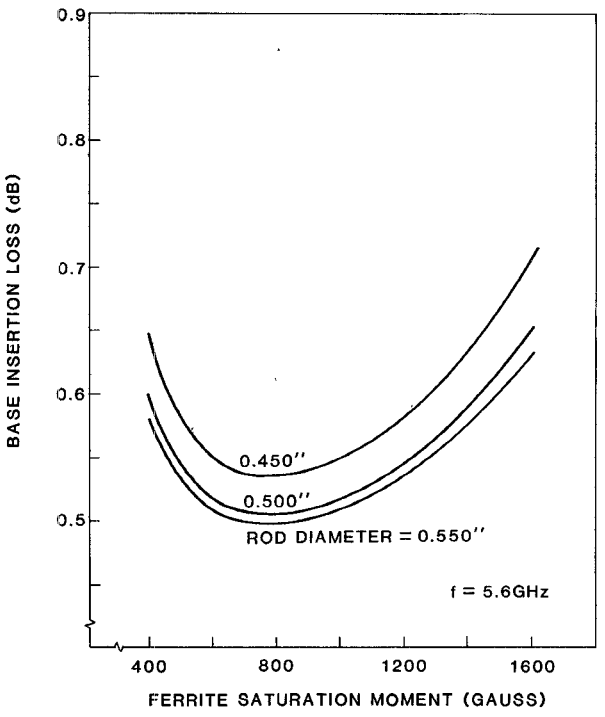

Fig. 7. *C*-band transverse-field dual-mode phase shifter loss dependence on saturation moment for selected rod diameters.

various levels of ferrite material saturation moment, where a maximum phase shift of 500° and a peak M/M_s value of 0.75 have been assumed for configurations incorporating 45° Faraday rotators at each end.

As a consequence of the dependence of length on diameter, an optimum diameter value exists which minimizes the

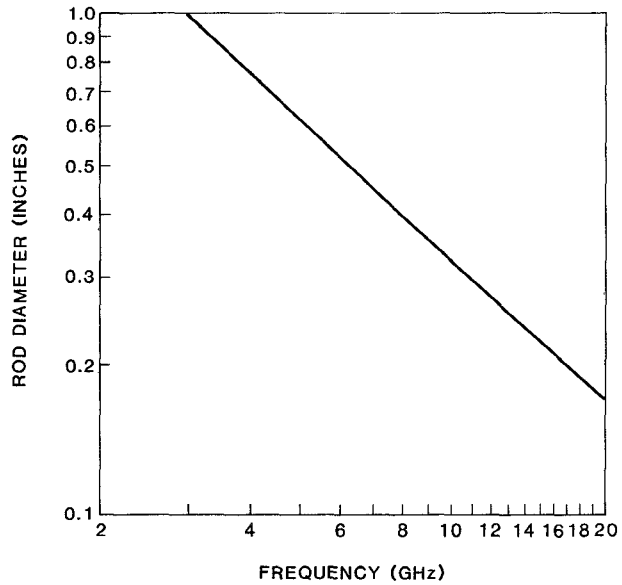

Fig. 8. Transverse-field dual-mode phase shifter optimum-loss rod diameter versus frequency.

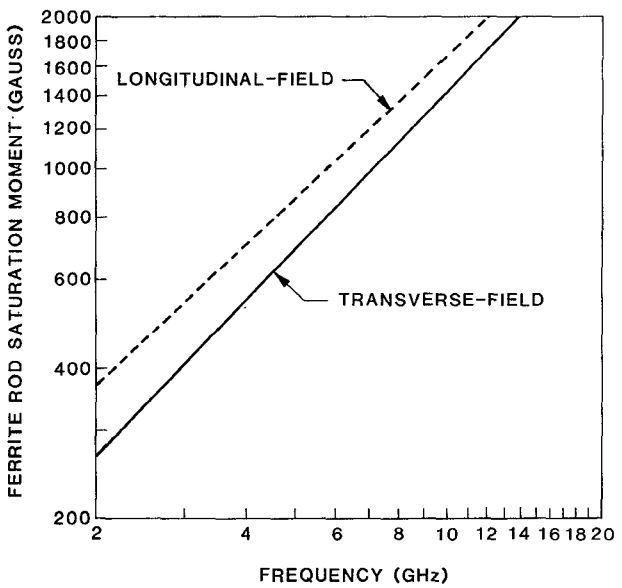

Fig. 9. Ferrite saturation moment versus frequency for loss-optimized dual-mode phase shifters.

insertion loss for a given ferrite material. For smaller diameters, the conductive, dielectric, and magnetic losses rise at a faster rate than the length reduction, and so the net loss increases; the opposite situation occurs as the diameter is increased above the optimum value, although the rate of increase tends to be more gradual. The existence of an optimum diameter value is in contrast with the longitudinal field dual-mode phase shifter, for which insertion loss decreases monotonically with diameter up to the point of onset of higher order modes that cannot be suppressed. Fig. 6 shows plots relating insertion loss to diameter for the previous C-band design. These computations were made using the same pertubational relationships and material property assumptions as in previous studies for longitudinal field configurations. In common with the

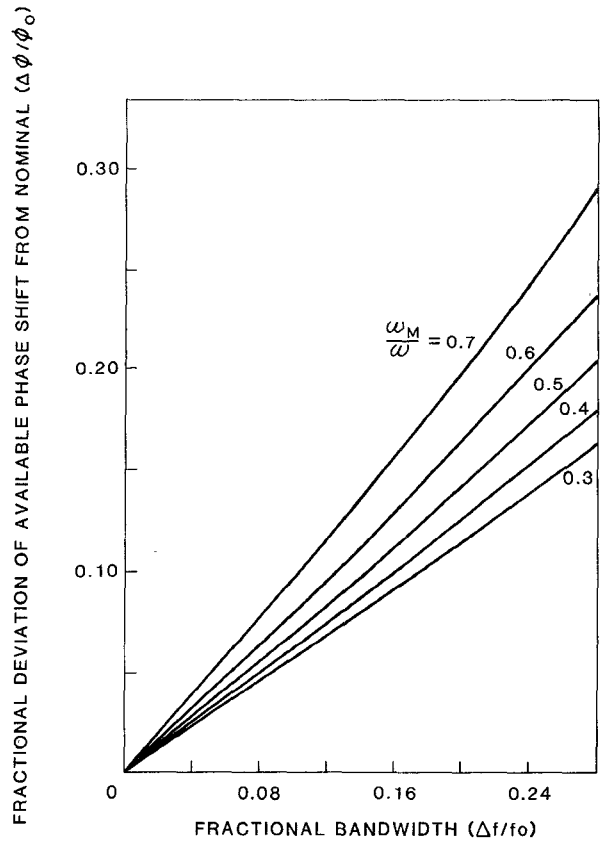

Fig. 10. Frequency dispersive deviation of available phase shift for transverse-field dual-mode ferrite phase shifter.

longitudinal field type, an optimum value for ferrite material saturation moment exists which minimizes insertion loss, although the value for the transverse field case is lower. Fig. 7 demonstrates the existence of this optimum value, giving curves of insertion loss versus saturation moment at selected rod diameters at C-band. In summary, Figs. 8 and 9 show optimum diameter and optimum saturation moment values as functions of frequency.

The transverse field interaction for a fully filled waveguide is generally more frequency dependent than the longitudinal field interaction; hence frequency dispersion of phase shift values will be greater. Fig. 10 shows a family of curves relating deviation of available band-edge phase shift from nominal as a function of fractional bandwidth for selected band-center ω_m/ω values. As with the longitudinal field case [6], modulation of insertion loss will occur with deviation of the polarizers or Faraday rotators, although the smaller frequency dependence of the latter will yield less band-edge modulation over the same frequency range. Hence, for the configuration using Faraday rotators, it appears that a smaller insertion loss modulation is exchanged for a greater dispersion of phase shift characteristics.

III. Switching Considerations

One of the important features of the dual-mode phase shifter is the fact that the switching wires and the latching yoke are removed from the microwave circuit. This results

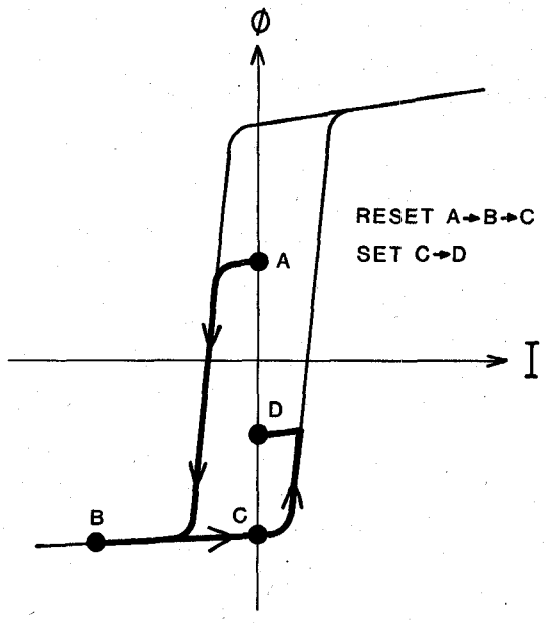

Fig. 11. Ferrite hysteresis loop showing switching cycle.

in fairly simple fabrication and assembly of the phase shifter. However, the switching performance of the device is affected by eddy currents induced in the waveguide walls whenever the magnetic flux of the bias field is changed to produce phase shift. Prior study [6] of the longitudinal field dual-mode phase shifter has shown energy increases dramatically when the switching time is reduced below a particular reference time, defined as the "shorted-turn" damping time constant, which is determined by the structure dimensions and by the resistivity and thickness of the waveguide walls. The transverse field dual-mode device exhibits similar behavior, but the reference time is significantly reduced compared with the longitudinal field device.

The switching cycle consists of a "reset" portion followed by a "phase set" portion, as indicated in Fig. 11. It is assumed that partial switching of the core is accomplished by controlling the volt–time integral of the driver output pulse. The following analysis determines switching energy as a function of switching time as the flux is changed from the maximum negative value to the maximum positive value.

Consider a ferrite rod which has been metallized to form a waveguide. Onto this is placed a winding of N turns and a latching yoke. This assembly may be modeled by the circuit shown in Fig. 12. Here R_c is the effective resistance of the ferrite core during switching, L is the inductance of the assembly, and R_{st} is the shorted-turn resistance of the waveguide metallization multiplied by N^2 to reflect its apparent value in the primary circuit of the N:1 transformer. To change the flux from its maximum negative remanent value to its maximum positive remanent value, a constant voltage V is applied for a time T. The energy to switch the ferrite is

$$W_H = 2B_{\max} H_c \Lambda \tag{15}$$

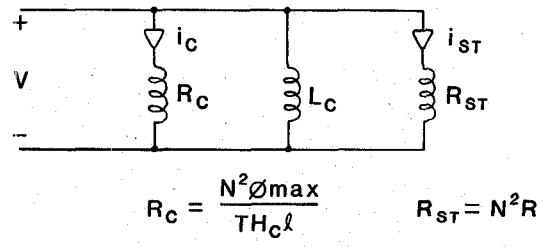

Fig. 12. Ferrite equivalent circuit during switching.

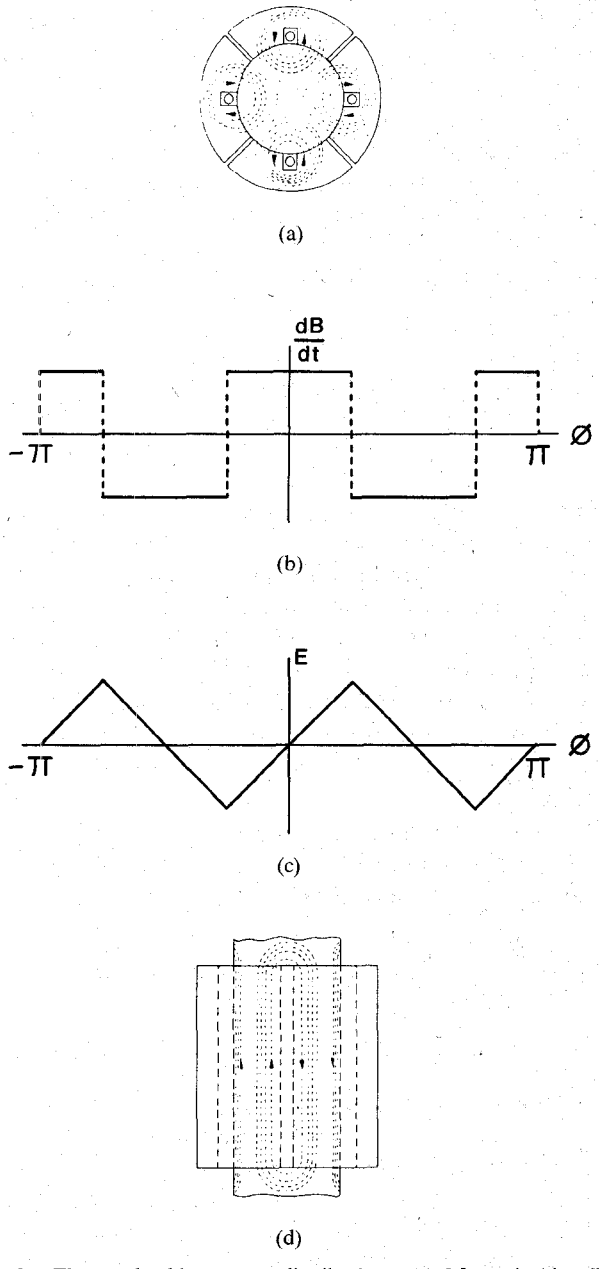

Fig. 13. Flux and eddy current distributions. (a) Magnetic bias flux distribution. (b) Spatial distribution of time rate of change of magnetic flux density. (c) Spatial distribution of induced electric field intensity. (d) Eddy current distribution.

where $B_{\max}$ is the maximum remanent flux density, H_c is the coercive force, and Λ is the volume of ferrite being switched. This may also be written $W_H = V^2 T / R_c$. The energy dissipated by the eddy currents may be written

$W = V^2T/R_{st}$ so that the total energy furnished is

$$W = W_H\left(1+\frac{R_c}{R_{st}}\right) = W_H\left(1+\frac{\tau}{T}\right) \tag{16}$$

where τ is the reference time, e.g. the shorted-turn damping time constant. The core resistance R_c is proportional to the square of the turns ratio, which means that the ratio of R_c to R_{st} is independent of the turns ratio. The effective resistance of the ferrite core may be adjusted through the turns ratio to present a wide range of levels to the electronic driver without changing the energy requirements, as long as the switching time T is held constant.

The length and the diameter of the switched ferrite are approximately the same for the transverse field device and the longitudinal field device. Let D represent the diameter of the microwave ferrite, l the length, S the thickness of the metallization, and ρ the resistivity of the metallization. The following are easily derived for the longitudinal field device:

$$R_c = \frac{\pi D^2N^2B_{\max}}{4TH_cl} \qquad R_{st} = \frac{\pi D^2N^2\rho}{sl} \qquad \tau = \frac{SDB_{\max}}{4\rho H_c}. \tag{17}$$

The distribution of the magnetic flux for the transverse-field device is shown in Fig. 13(a). During switching the spatial distribution of the time rate of change of the magnetic flux density is shown in Fig. 13(b). This results in an induced electric field intensity as shown in Fig. 13(c) and eddy currents as shown in Fig. 13(d). The current density is obtained from the electric field intensity through multiplying by the conductivity of the waveguide walls. The total eddy currents are found by integrating the current density.

Let N be the number of turns in a single slot of the yoke. Utilizing the fourfold symmetry of the geometry, the resistances and time constant may be calculated to be

$$R_c = \frac{\pi N^2lB_{\max}}{4TH_c} \qquad R_{st} = \frac{32N^2\rho l}{\pi SD} \qquad \tau = \frac{\pi^2SDB_{\max}}{128\rho H_c}. \tag{18}$$

The fringing fields at either end of the yoke have been ignored in the calculation of the shorted-turn resistance. However, these will increase the shorted-turn resistance so that the shorted-turn time constant of (18) represents an upper bound. The shorted-turn time constant of (17) represents a lower bound for the longitudinal field case since fringing fields will lower the shorted-turn resistance for that geometry. Equations (17) and (18) imply that the shorted-turn damping constant for the transverse field device may be about 30 percent of that for the longitudinal field device. Consequently, a switching time for the transverse-field device equal to 30 percent or less of the time for an equivalent-geometry longitudinal-field type should produce the same shorted-turn energy dissipation.

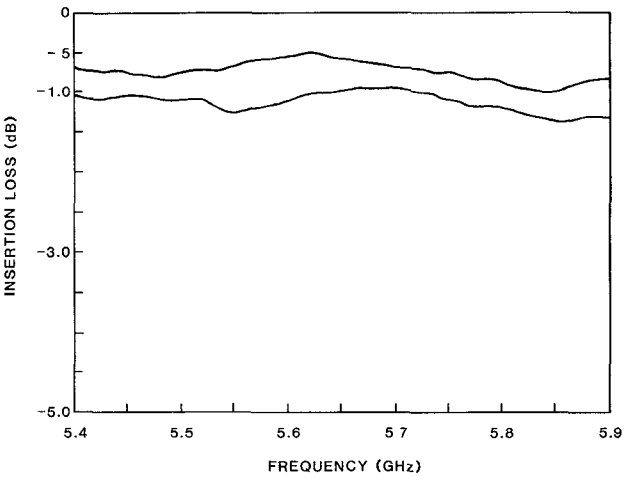

Fig. 14. Insertion loss envelope versus frequency.

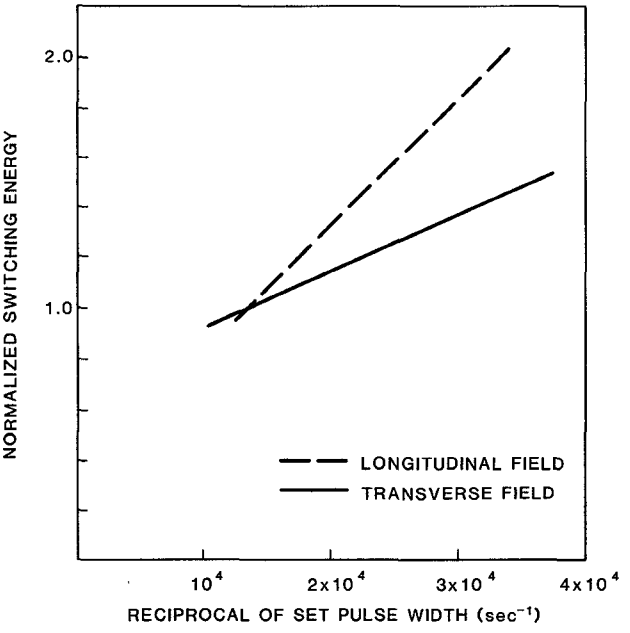

Fig. 15. Switching energy as a function of the reciprocal of switching time.

IV. Experimental Verification

To validate the theory, a phase shifter was fabricated at C-band. The basic design was that of longitudinal-field dual-mode unit using a saturation magnetization of 1200 G and a rod diameter of 0.480 in. The rod was fitted with yokes and tested as a longitudinal-field unit. The yokes were removed and new yokes designed to establish a transverse-field unit. The insertion loss envelope, as the phase shifter is switched between the various states, is shown in Fig. 14.

The measurement of switching energy was made during the set cycle. The phase shifter was saturated with a reset pulse. The drive voltage was then varied while holding the volt–time product constant, and the average current was measured. The product of average current and volt–time product yields the switching energy. The switching energy was normalized to that obtained for a switching time of 75 μs and then plotted versus the reciprocal of the set pulse

width ($1/T$). According to (16) this will yield a straight line whose slope is the shorted-turn time constant. This is shown in Fig. 15, which clearly indicates that the transverse-field device has a shorted-turn time constant that is lower by about a factor of 2.25.

V. Conclusions

A new type of dual-mode phase shifter has been described. This phase shifter uses a transverse magnetic field in the differential phase shift region. Because of the distribution of the bias field, the waveguide wall eddy currents are reduced, which results in a reduced shorted-turn damping time constant when compared with the conventional dual-mode unit using a longitudinal magnetic bias field.

Analysis of the RF performance of the phase shifter was presented. This analysis indicates that the transverse-field device exhibits an optimum value of saturation magnetization which minimizes the insertion loss and that this value is considerably less than that of the longitudinal-field device. Unlike the longitudinal-field device, whose diameter is limited by the onset of higher order modes, the transverse-field device exhibits an optimum diameter which minimizes insertion loss.

References

[1] C. R. Boyd, Jr., "A dual-mode latching reciprocal ferrite phase shifter," *IEEE Trans. Microwave Theory Tech.*, vol. MTT-18, pp. 1119–1124, Dec. 1970.

[2] R. G. Roberts, "An *X*-band reciprocal latching Faraday rotator phase shifter," in *IEEE Int. Microwave Symp. Dig.*, May 1970, pp. 341–345.

[3] C. R. Boyd, Jr., "Design of ferrite differential phase shift sections," in *IEEE Int. Microwave Symp. Dig.*, May 1975, pp. 240–242.

[4] C. R. Boyd, Jr., "A transmission line model for the lossless nonreciprocal waveguide," in *Proc. Int. Symp. Microwave Technology in Industrial Development* (Brazil), July 1985, pp. 209–216.

[5] J. J. Green and F. Sandy, "Microwave properties of partially magnetized ferrites," Rome Air Development Center, Rome, NY Final Report. RADC-TR-69-338, Sept. 1969.

[6] C. R. Boyd, Jr., "Comments on the design and manufacture of dual-mode reciprocal latching ferrite phase shifters," *IEEE Trans. Microwave Theory Tech.*, vol. MTT-22, pp. 593–601, June 1974.

✠

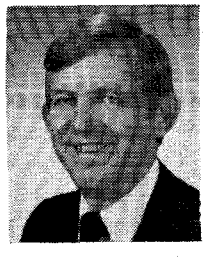

William E. Hord (S'57–M'69–SM'78) was born in Leola, SD, in 1938. He received the B.S.E.E. degree from the Missouri School of Mines and Metallurgy, Rolla, in 1959 and the M.S.E.E. degree in 1963 and the Ph.D. degree in 1966 from the University of Missouri at Rolla.

His teaching experience is as an Instructor of Electrical Engineering from 1960 to 1966 at the University of Missouri at Rolla, a part-time Assistant Professor at the Graduate Engineering Center, University of Missouri at Rolla during 1967–1968, and Professor of Engineering at Southern Illinois University. At SIU he was Chairman of the Department of Engineering from 1974 to 1981 and Acting Dean of the School of Engineering from 1983 to 1984. Dr. Hord worked at the Sperry Gyroscope Company from 1959 to 1960 on the development of high-power klystrons. From 1966 to 1968 he worked at the Emerson Electric Company on the development of airborne phased-array antenna, in particular, the RARF antenna. In 1984 he joined the Microwave Applications Group, where he is presently Vice President of Engineering.

Dr. Hord is a member of Eta Kappa Nu, Phi Kappa Phi, Sigma Xi, and Tau Beta Pi. He was named Outstanding Electrical Engineering Teacher in IEEE Region 5 in 1984. He currently serves as Co-Chairman of the MTT Technical Committee on Microwave Ferrites.

✠

Charles R. Boyd, Jr. (F'85) received the B.S.E.E. degree from Carnegie Mellon University, Pittsburgh, PA, in 1953 and the M.E.E. and PH.D. degrees in electrical engineering from Syracuse University, Syracuse, NY, in 1962 and 1964, respectively. He is also a graduate of the General Electric Company's Advanced Courses in Engineering, a three-year program of part-time graduate level studies, which he completed in 1959.

From 1953 to 1956 he was a Field Engineer with Westinghouse Electric Corporation, where he worked on developmental auto-pilot and side-looking radar equipment. In 1956 he joined General Electric, Utica, NY, where he helped design a missile transponder for the early Atlas guidance system. He transferred to the General Electric Electronics Laboratory, Syracuse, NY, in 1957, and carried out development of advanced microwave semiconductor and ferrite circuits. From 1961 to 1962 he was on academic leave at Syracuse University, and from 1962 to 1963 he supervised and taught a portion of the General Electric Advanced Courses in Engineering, returning in each case to active work at the General Electric Electronics Laboratory. In 1965 he joined the Rantec Division of Emerson Electric, Calabasas, CA, where he managed an engineering group engaged in development and design of microwave solid-state components. He was on the faculty of the University of California, Los Angeles, from 1967 to 1970. He founded Microwave Applications Group, Santa Maria, CA, in 1969, and has since served as its President.

Dr. Boyd received the 1982 Microwave Applications Award from the Microwave Theory and Techniques Society of that organization for his work on ferrite phase control components.

✠

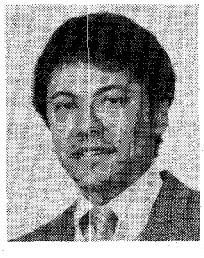

Daniel Diaz was born in New York City, NY, on September 21, 1953. He was graduated from the Saunders Trades and Technical High School in Yonkers, NY. Following high school he enlisted in the U.S. Navy and served as an Electrician. He received the B.S.E.E. degree from California State University at Fresno in 1985.

He worked in the antenna laboratory of the Radar Systems Group of Hughes Aircraft Company during the summer of 1985. In January 1986 he joined Microwave Applications Group, Santa Maria, CA, where he is working on the development of ferrite phase shifters and control circuits.